Chapter 15

Laser Ablation of Polymethylmethacrylate (PMMA) by Phase-Controlled Femtosecond Two-Color Synthesized Waveforms

Ci-Ling Pan, Chih-Hsuan Lin, Chan-Shan Yang and Alexey Zaytsev

Additional information is available at the end of the chapter

http://dx.doi.org/10.5772/65637

Abstract

Single-shot laser ablation of polymethylmethacrylate (PMMA) was studied using dual-color waveform synthesis of the fundamental (ω) and its second harmonic (2ω) of a femtosecond Ti: Sapphire laser. Changing the relative phase of the fundamental (ω) and second-harmonic (2ω) outputs of the exciting laser resulted in clear modulation of the ablated area. The modulation as well as the dependence of the ablation threshold on the relative phase between the ω and 2ω beams correlated closely with the theoretical model of laser breakdown (ablation) of transparent materials through photoionization in the intermediate regime (Keldysh parameter $\gamma \approx 1.5$). Our study illustrates the potential applications of using phase-controlled synthesized waveform for laser processing of materials.

Keywords: femtosecond pulses, laser ablation, coherent control, breakdown, polymethylmethacrylate (PMMA), polymer, Keldysh parameter

1. Introduction

Femtosecond (fs) laser micromachining has been studied intensively for the past two decades. One of the advantages of using ultrashort laser pulses rather than longer pulses for laser material processing pertains to the nonthermal ablation mechanism. By considerably reducing the area of heat-affected zones, precise laser micro- and nanomachining have become feasible for fs machining. To date, fs laser micromachining has been performed on a variety of wide-

band-gap materials, such as polymers [1, 2], fused silica [3–6], and silicon [7–10]. However, almost all of these studies employed one-color laser pulses. More recently, coherent waveform-synthesized two-color laser pulses have been successfully used for increasing plasma generation [11], generating high harmonics [12], and producing broadband terahertz radiation [13]. By studying femtosecond laser ablation of polymethylmethacrylate (PMMA), our group demonstrated that the ablated hole areas exhibited clear modulation with a contrast of 22% by varying the relative phase between the ω and 2ω beams [14]. It was assumed that different peak intensity for the synthesized waveform was responsible for the observed phenomena. The physical mechanism was not clear.

In general, ultrafast laser ablation of dielectrics, such as PMMA, has been explained by the photochemical, photothermal, and photophysical models [15]. In the photochemical model, direct bond breaking in PMMA is achieved by exposing it to an ultrashort laser pulse for producing several reaction products, such as CO, CO_2, CH_4, CH_3OH, and $HCOOCH_3$. In the photothermal model, electronic excitation by picosecond laser pulses results in thermal bond breaking, leading to the formation of PMMA monomers. Among these models, the most interesting one is the photophysical one, in which both thermal and nonthermal bond breaking occur simultaneously. In thermal bond breaking, electronic excitation by ultrashort laser pulses results in ultrashort-laser-induced ionization in the picosecond (ps) and fs ranges. The three main processes of photophysical laser-induced breakdown are (i) excitation of conduction band electrons through ionization, (ii) heating of conduction band electrons through irradiation of the dielectric, and (iii) plasma energy transfer to the lattice, which causes bond breaking [16–19].

The Keldysh formalism, describing electron tunneling through a barrier created by the electric field of a laser, is often employed for modeling laser breakdown of materials by photoionization, including both multiphoton and tunneling cases. The Keldysh parameter can be expressed as the square root of the ratio between the ionization potential and twice the value of the ponderomotive potential of the laser pulse. Alternatively, it can be expressed as the ratio of tunneling frequency to the laser frequency. The tunneling time or the inverse of the tunneling frequency is given by the mean free time of an electron passing through a barrier width, $l_{\text{tunneling}} = I_p/eE(t, \varphi)$, where I_p is the ionization potential, e is the electron charge, and $E(t, \varphi)$ is the optical field.

Depending on the laser intensity used for above-threshold ionization [20–22], two regions of photoionization exist: the tunneling ionization region [20, 23, 24] and multiphoton ionization region [25–28]. In tunneling ionization, the electric field is extremely strong. The Coulomb well can be suppressed to cause the bound electron to tunnel through the barrier and be ionized. At lower laser intensities, the electron can absorb several photons simultaneously. The electron makes the transition from the valence band to the conduction band if the total energy of the absorbed photons is greater than or equal to the band gap of the material.

The boundary between tunneling ionization and multiphoton ionization is unclear. Schumacher et al. showed that there should be a so-called intermediate region that exhibit both tunneling and multiphoton characteristics. Mazur et al., following the Keldysh formalism, estimated that the intermediate region corresponded to a Keldysh parameter $\gamma \approx 1.5$ [29].

http://dx.doi.org/10.5772/65637

The tunneling ionization rate is a function of the electric field. It is well known that the multiphoton ionization rate can be expressed as $\omega_{mpi} \propto \sigma_k I^k$, where I is the laser intensity and σ_k is the multiphoton absorption coefficient for k photons [30]. When the ionization occurs in the intermediate region, an electron can absorb several photons and be ionized by the tunneling effect. In this regime, the ionization rate can also vary with phase of the exciting electric field. The laser intensity required, however, is considerably lower than that in the pure tunneling ionization case.

In this chapter, we present the current progress on laser ablation of polymethylmethacrylate (PMMA) by phase-controlled femtosecond two-color synthesized waveforms. Significantly, laser breakdown (ablation) of transparent materials through photoionization in the intermediate regime (Keldysh parameter $\gamma \approx 1.5$) was demonstrated for the first time. The modulation of ablated hole area as well as the dependence of the ablation threshold on the relative phase between the ω and 2ω beams were observed. The data correlated closely with the theoretically predicted phase dependence of the photoionization rate using the Keldysh formalism.

2. The physical mechanisms of ultrafast laser ablation

2.1. Introduction

In this section, some key concepts of ultrafast laser ablation will be summarized. This includes light-matter interaction mechanisms such as photochemical, photothermal and photophysical. Dielectric breakdown due to ionization by tunneling, multiphoton and avalanche processes are described. Most relevant for this work, the so-called intermediate regime of photoionization, will be formulated by using the Keldysh equation, defining the Keldysh parameter used throughout this chapter.

2.2. Photoexcitation processes

Laser ablation is one of the manifestations of light-matter interactions. As expected, the ablation processes depend on characteristics of the irradiating laser, such as its intensity, wavelength, and polarization. When ultrafast laser are used, ablation mechanism become more complicated. For polymeric materials, not only photoionization but also the direct bond breaking will lead the ablation process. The main mechanisms are photochemical, photothermal, and photophysical. These three effects are located in different regions of laser pulse.

For ultrafast laser ablation of PMMA, there are two dominant mechanisms, i.e., photochemical and photothermal. In photochemical events, absorption of photons by the material being processed lead directly to covalent bond breaking [15]. The polymeric materials, such as PMMA, are generally made of a wide variety of chromophores, which may dissociate into reactive fragments by absorption of energetic UV photons. Absorption of less energetic photons, e.g., those in the visible or near infrared band, can also lead to the above photochemical processes [15]. Photothermal effect is another basic mechanism of laser ablation. Irradiated by ultrashort laser pulses, the irradiated material absorbs photons and transfer energy to

electrons such that photoionization of the material can occur. In this case, excited electrons can heat up the lattice and induce bond breaking [15]. Depending on fluence of the irradiating laser, ablation could be originated through either tunneling ionization or above-threshold ionization (ATI). Multiphoton and avalanche ionization are two main mechanisms of ATI.

In a large band gap material, it is difficult to ionize the constituent atoms by absorbing only one photon from commonly available lasers. Theoretically, an atom might absorb two or more photons simultaneously, giving electrons sufficient energy to cross the band gap from the valence band to the conduction band. This is illustrated schematically in **Figure 1**. For multiphoton ionization to occur, the laser intensity needs to be in the range of 10^{12} –10^{16} W/cm^2. In contrast, the avalanche ionization mechanism, for which the laser intensity required is in the range of 10^{9} –10^{12} W/cm^2, depicts the process whereas a small number of initial electrons of the materials are accelerated to a high value of kinetic energy. Afterwards, high-energy electrons will collide with another electron of lower energy, which is shown schematically in **Figure 1**. Afterwards, the two electrons are accelerated by the laser field collide with other electrons in an avalanche-like process, leading to large amount of electrons with high energies to form a plasma.

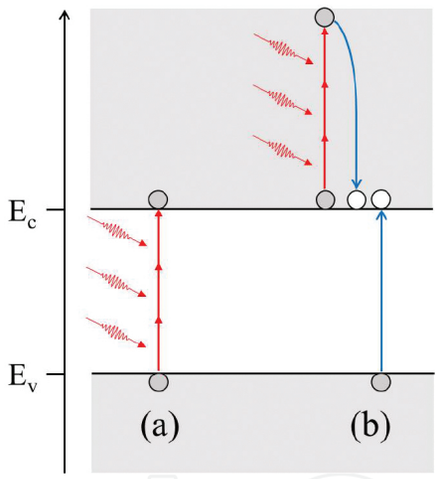

Figure 1. Schematic diagrams illustrating the processes of (a) multiphoton ionization and (b) avalanche ionization of materials.

Finally, in the photophysical mechanism, nonthermal, photochemical, thermal, and photothermal processes all play their respective roles. Two independent mechanisms of bond breaking could be present. Further, bond breaking energies for the ground state and the excited state chromophores are, in general, different. The photophysical mechanism of ablation usually applies for irradiating lasers with short laser pulses, of which the pulse duration is in the ps and fs range.

2.3. Basics of femtosecond ablation dynamics of PMMA in the intermediate regime

In a class paper, Keldysh showed that the total photoionization rate of a material upon irradiation by a laser can be written as [31, 32]:

http://dx.doi.org/10.5772/65637

$$\varpi = \frac{2\omega}{9\pi}\left(\frac{\sqrt{1+\gamma^2}}{\gamma}\frac{m\omega}{\hbar}\right)^{3/2} Q\left(\gamma, \frac{\tilde{\Delta}}{\hbar\omega}\right)\exp\left\{-\pi < \frac{\tilde{\Delta}}{\hbar\omega}+1 > \right.$$
$$\left.\times\left[K\left(\frac{\gamma}{\sqrt{1+\gamma^2}}\right) - E\left(\frac{\gamma}{\sqrt{1+\gamma^2}}\right)\right] / E\left(\frac{1}{\sqrt{1+\gamma^2}}\right)\right\} \tag{1}$$

where $\gamma = \omega(mI_p)^{1/2}/eF$ is the so-called Keldysh parameter, ω is laser frequency, m is the electronic mass, e is the electronic charge, $\hbar$ is plank constant, and $\tilde{\Delta}$ is the effective ionization potential,

$$\tilde{\Delta} = \frac{2}{\pi} I_p \frac{\sqrt{1+\gamma^2}}{\gamma} E\left(\frac{1}{\sqrt{1+\gamma^2}}\right). \tag{2}$$

The symbol $< \tilde{\Delta}/\hbar\omega + 1 >$ in Eq. (1) is the integer part of the number, $\tilde{\Delta}/\hbar\omega + 1$, while $Q(\gamma, \tilde{\Delta}/\hbar\omega)$ is defined by Eq. (3):

$$Q\left(\gamma, \frac{\tilde{\Delta}}{\hbar\omega}\right) = \sqrt{\frac{\pi}{2K\left(1/\sqrt{1+\gamma^2}\right)}}$$
$$\times\sum_{n=0}^{\infty}\exp\left\{-\pi n\left(K\left(\gamma/\sqrt{1+\gamma^2}\right) - E\left(\gamma/\sqrt{1+\gamma^2}\right)\right) / E\left(1/\sqrt{1+\gamma^2}\right)\right\}$$
$$\times\Phi\left\{\sqrt{\frac{\pi^2\left(2 < \frac{\tilde{\Delta}}{\hbar\omega}+1 > -2\frac{\tilde{\Delta}}{\hbar\omega}+n\right)}{2K\left(1/\sqrt{1+\gamma^2}\right)E\left(1/\sqrt{1+\gamma^2}\right)}}\right\}, \tag{3}$$

where K and E are first and second kind of the complete elliptic integrals and Φ is the Dawson integral.

In the presence of high-intensity or strong electric field of the laser, we are in the region of tunneling ionization or $\gamma << 1$. The rate of tunneling ionization is given by

$$\varpi_{\text{tunneling}} = \frac{2}{9\pi^2}\frac{I_p}{\hbar}\left(\frac{mI_p}{\hbar^2}\right)^{3/2}\left(\frac{e\hbar F}{m^{1/2}I_p^{3/2}}\right)^{5/2}$$
$$\times\exp\left\{-\frac{\pi}{2}\frac{m^{1/2}I_p^{3/2}}{e\hbar F}\left(1-\frac{1}{8}\frac{m\omega^2 I_p}{e^2F^2}\right)\right\}. \tag{4}$$

On the other hand, if $\gamma >> 1$, the ionization is in the regime of multiphoton absorption. The probability of multiphoton absorption is given by

$$\varpi_{\text{multiphoton}} = \frac{2}{9\pi}\omega\left(\frac{m\omega}{\hbar}\right)^{3/2}\Phi\left[\sqrt{2<\frac{\tilde{\Delta}}{\hbar\omega}+1>-\frac{2\tilde{\Delta}}{\hbar\omega}}\right]$$
$$\times\exp\left\{2<\frac{\tilde{\Delta}}{\hbar\omega}+1>\left(1-\frac{e^2F^2}{4m\omega^2I_p}\right)\right\}\left(\frac{e^2F^2}{16m\omega^2I_p}\right)^{<\tilde{\Delta}/\hbar\omega+1>}. \quad (5)$$

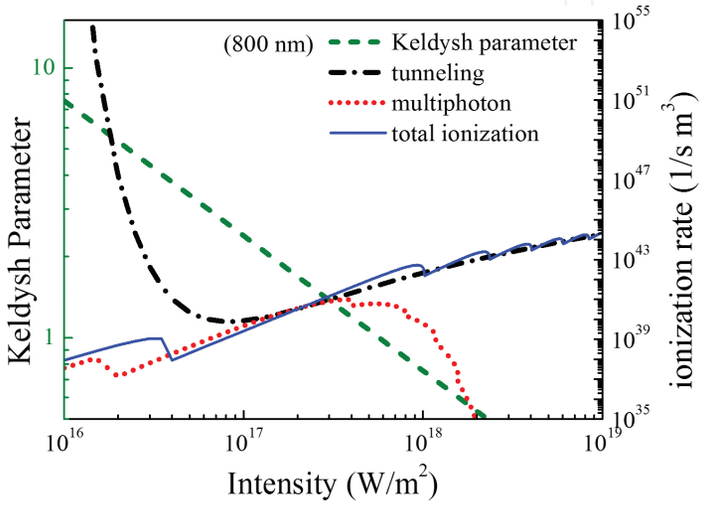

Figure 2. The photonionization rate and Keldysh parameter are plotted as a function of laser intensity (λ = 800 nm) in PMMA.

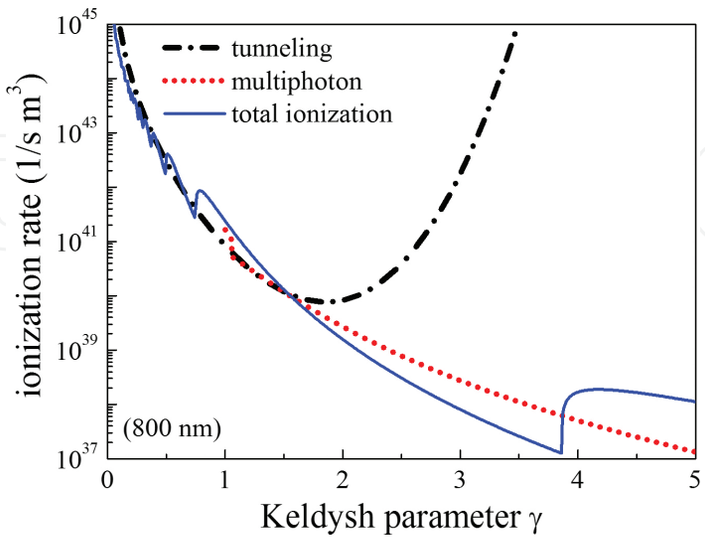

Figure 3. Photonionization rates are plotted as a function of the Keldysh parameter for NIR (λ = 800 nm) ultrafast laser ablation of PMMA.

http://dx.doi.org/10.5772/65637

Below, we have plotted the effective ionization potential $\tilde{\Delta} = \Delta + e^2F^2/4m\omega^2$ and the Keldysh parameter as a function of laser intensity in PMMA in **Figure 2**. The laser wavelength is assumed to be in the near infrared (λ = 800 nm). Besides the total ionization rate, contributions by tunneling and multiphoton ionization, respectively, are also shown. The dependence of the photoionization rate on the Keldysh parameter is also enlightening. This is illustrated in **Figure 3**. Similar curves for ultrafast laser ablation of PMMA using NUV (λ = 400 nm) are presented in **Figures 4** and **5**.

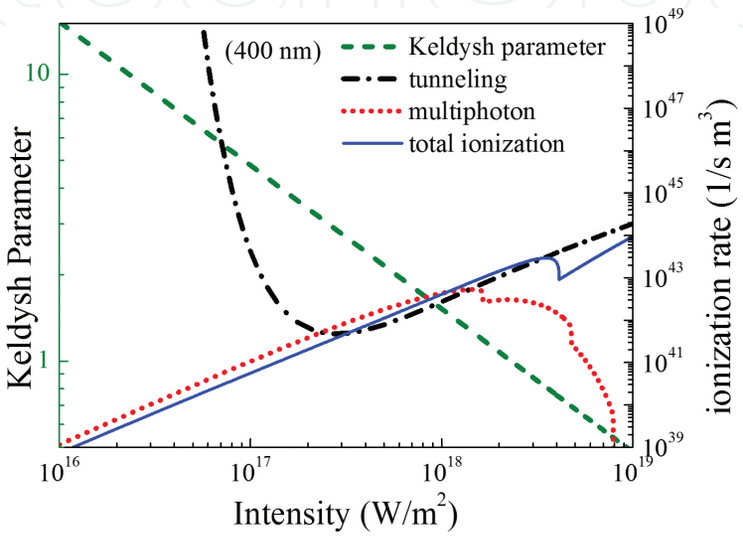

Figure 4. Photonionization rates and Keldysh parameter are plotted as a function of laser intensity for NUV (λ = 400 nm) laser ablation of PMMA.

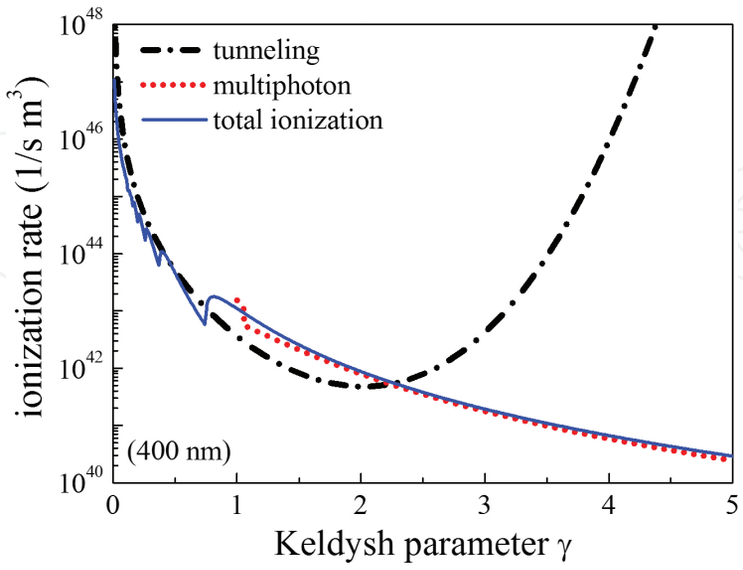

Figure 5. Photonionization rates are plotted as a function of the Keldysh parameter for NUV (λ =400 nm) ultrafast laser ablation of PMMA.

The solid blue lines in **Figures 2–5** correspond to the photoionization rate of PMMA calculated using Eq. (1). The full expression of Keldysh formula (Eq. 1) take into account both tunneling and multiphoton ionization processes. The dashed black line and dotted red line represent the tunneling ionization and multiphoton ionization rates determined from Eqs. (4) and (5), respectively. When the Keldysh parameter, $\gamma \approx 1.5$, tunneling and multiphoton ionization rates overlap each other for PMMA irradiated with either NIR (800 nm) or NUV (400 nm) beams. We defined this overlapping region as an intermediate regime. To predict the ionization rate in the intermediate regime, we assume the process resembles that of tunneling ionization. The ionization rate depends on the instantaneous field amplitude, $F_L(t)$, which is given by [22]:

$$\varpi(t) = 4I_p^{5/2} \frac{1}{F_L(t,\varphi)} \exp\left(-\frac{2}{3} I_p^{3/2} \frac{1}{F_L(t,\varphi)}\right) \tag{6}$$

In order to understand the phase dependence of observed dual-color laser ablation phenomena, we proceed as follows: assume that the irradiating laser consists of beams at two commensurate laser frequencies, i.e., the fundamental (ω) laser beam and its second harmonic (2ω). The dual-color laser field $F(t)$ can then be written as

$$F_L(t,\varphi) = F_\omega e^{-2\ln 2t^2/\tau^2} \cos\omega t + F_{2\omega} e^{-2\ln 2t^2/\tau^2} \cos(2\omega t + \varphi) \tag{7}$$

where F_ω and $F_{2\omega}$ are the envelope function of the fundamental and second-harmonic laser fields, respectively; φ is the relative phase of the second-harmonic (2ω) beam with respect to that of the fundamental (ω) beam.

The Keldysh model above can be used to describe the photoionization phenomenon due to either the multiphoton or tunneling route. Typically, the Keldysh parameter is defined by the square root of the ratio of ionization potential and twice the ponderomotive potential of the laser pulse. Some researchers also define it as the ratio of tunneling frequency to the laser frequency [33]. In the original derivation, the Keldysh parameter was used to describe the phenomenon of an electron tunneling through a barrier created by the optical field. The tunneling time or the inverse of the tunneling frequency is determined by the mean free time of the electron passing through a barrier width l.

$$l_{\text{tunneling}} = I_p / eF_L(t,\varphi) \tag{8}$$

where I_p is the ionization potential, e is the electron charge and $F_L(t,\varphi)$ is the electric field of the incident laser. The average velocity of an electron can be written as,

$$< v >= \sqrt{\frac{2I_p}{m_e}}, \tag{9}$$

http://dx.doi.org/10.5772/65637

where m_e is the mass of an electron. By combining Eqs. (8) and (9), the tunneling time is given by

$$t_{\text{tunneling}}(t,\varphi) = \frac{l}{<v>} = \frac{\sqrt{I_p m_e}}{\sqrt{2} e F_L(t,\varphi)} = \frac{1}{\nu_{\text{tunneling}}(t,\varphi)} \tag{10}$$

Tunneling can occur if the mean tunneling time, which is given by Eq. (10), is less than half the period of the laser. Taking this into account, we modify the Keldysh parameter, γ as appropriate for this study as

$$\gamma = \frac{2t_{\text{tunneling}}}{t_{\text{laser}}} = \frac{l_{\text{tunneling}}}{l_{\text{laser}}} = \nu_{\text{laser}} \frac{\sqrt{2I_p m_e}}{eF_L(t,\varphi)} \tag{11}$$

where t_{laser} is the period of laser, l_{laser} is the mean distance that an electron moves during half of period t_{laser} at a mean velocity of <v>, and v_{laser} is the laser frequency. When the Keldysh parameter γ has relative phase dependence at dual-color synthesized waveform condition, the ionization rate can be calculated after we determine the effective frequency of the dual-color laser pulse.

For the purpose of defining the envelope equation for single-cycle pulse of the synthesized waveform, we express the complex electric field as [34]

$$E(t) = \tilde{E}_a(t) e^{-i\omega_0 ' t + i\psi} + c.c. = \tilde{E}(t) + c.c. = \frac{1}{\sqrt{2\pi}} \int_0^\infty \tilde{E}(\omega) e^{-i\omega t} d\omega + c.c., \tag{12}$$

where ω_0 is the effective carrier frequency denoted as

$$\omega_0 = \frac{\int_0^\infty \omega |E(\omega)|^2 d\omega}{\int_0^\infty |E(\omega)|^2 d\omega} \tag{13}$$

In Eqs. (12) and (13), $E(\omega)$ is the Fourier transform of $E(t)$ and ψ is the imaginary part of the complex envelope. Substituting the effective carrier frequency into Eq. (1), we can plot the photoionization rate as a function of laser intensity and the relative phase between the fundamental (ω) and second-harmonic (2ω) beams in our experiment, which is shown in **Figure 6**.

According to **Figure 6**, the ionization rate is predicted to be dependent on the relative phase of the fundamental (800 nm) and second-harmonic (400 nm) beams. Further, the modulation of ionization rate is more pronounced at higher laser intensities.

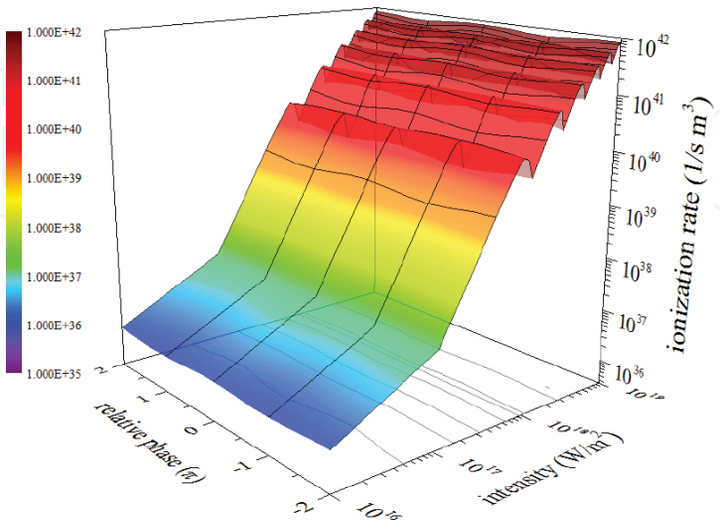

Figure 6. The total ionization rate versus laser intensity and relative phase of fundamental (ω) and second-harmonic (2ω) laser beams.

Recall that ablation by a laser with low and high intensities would fall into the regimes governed by multiphoton and tunneling ionization mechanisms, respectively. Conventionally, tunneling ionization corresponds to a regime in which the Keldysh parameter $\gamma << 1$. In this limit, the strength of the field is more than the value necessary to overcome the barrier. For a weaker field such that the Keldysh parameter $\gamma >> 1$, the main mechanism for ionization is due to the multiphoton ionization. In this regime, the electric filed strength is below the value that required for overcoming the barrier. In order to calculate the Keldysh parameter for the dual-color case, we need to define the period of the laser t_{laser}. It can be easily shown that the period of dual-color synthesized waveform by NIR (800 nm) and NUV (400 nm) beams is essentially that of the period of fundamental (ω) beam. Therefore, Eqs. (1) and (11) can be combined to determine the ionization rate as shown in **Figure 6**.

In the intermediate ionization regime, which is defined by $\gamma \approx 1.5$, the ionization rate has a strong phase dependence. Likewise, the electron tunnel time now depends on the phase difference between the two colors. Note that the electric field is actually lower than the value required for electrons to overcome the barrier.

Ablation threshold is an important parameter for laser material processing. It is a function of the laser pulse duration, wavelength, and intensity. According to the simplified Fokker-Planck equation [35]:

$$\frac{\partial n}{\partial t} = \beta(I)n + P(I), \tag{14}$$

http://dx.doi.org/10.5772/65637

where n is the free electron number, β is the avalanche ionization factor, assuming that the photogenerated electron distribution grows in magnitude without changing its shape. $P(I)$ is the multiphoton ionization rate. It can be approximated by the tunneling ionization rate by using Keldysh equation.

First of all, we need to calculate the number of free electrons generated by the laser pulse, assumed to be Gaussian in shape, $I(t) = I_0\exp(-4\ln 2t^2/\tau^2)$, where τ is the pulse duration. By solving the equation above, the free electron number can be obtained as

$$n = n_0 \exp\left(\int_0^\infty \beta dt\right) = n_0 \exp\left(\alpha \int_0^\infty I dt\right) = n_0 \exp\left(\alpha I_0 \int_0^\infty e^{-4\ln 2 t^2/\tau^2} dt\right) = n_0 \exp\left(\frac{\alpha I_0 \tau}{4}\sqrt{\frac{\pi}{\ln 2}}\right) \quad (15)$$

where α is the absorption coefficient of the material and n_0 is the total number of free electrons which is generated through multiphoton or tunneling ionization mechanism,

$$n_0 = \int_{-\infty}^{\infty} P(I) dt \quad (16)$$

The ablation threshold, F_{th}, can then be written as

$$F_{th} = \frac{2}{\alpha}\ln\left(\frac{n_{cr}}{n_0}\right) \quad (17)$$

where the density of free electrons, n_{cr} correspond to the threshold fluence, F_{th}. For ablation with ultrafast laser pulses, contribution by the avalanche ionization mechanism is not significant. Dielectric breakdown or ablation is through the processes of photoionization by tunneling and multiphoton ionization mechanisms. When the free electron number increases, the ablation threshold decreases.

3. Experimental methods

The experimental setup for laser ablation by dual-color femtosecond synthesized waveform [14] is shown schematically in **Figure 7**. The laser source was an amplified Ti: Sapphire laser system (Spitfire, Spectra Physics), which generates 70 fs laser pulses at a central wavelength of 800 nm (λ_1) with an energy up to 1.5 mJ at 1 kHz.

As shown in **Figure 7**, we adopt an inline arrangement for phase control of the fundamental and second harmonic of the laser output. The 800-nm fs pulses were focused onto the sample surface by a single convex lens with a focal length of 300 mm. Meanwhile, the fundamental beam frequency was doubled in a 100-μm-thick type-I Beta Barium Borate (β-BBO) crystal in

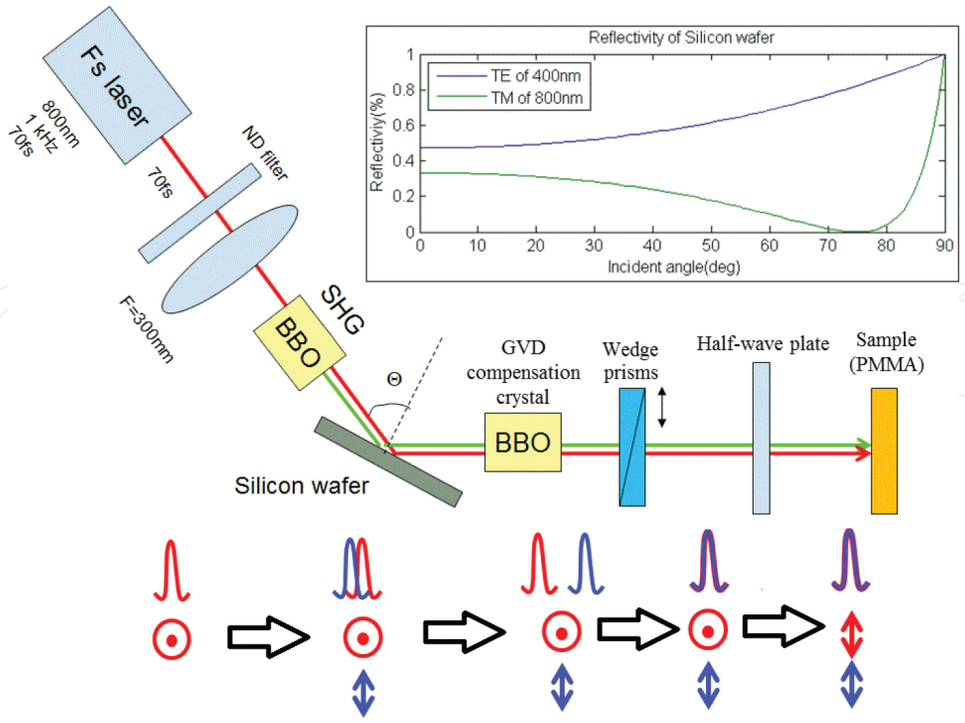

Figure 7. Experimental setup for laser ablation of PMMA by femtosecond dual-colour synthesized waveforms. The polarizations of fundamental and second harmonic pulses were controlled by the half-wave plate. ND: neutral density filter; BBO: Barium borate; GVD: group velocity dispersion. The inset shows the reflectivity of the silicon wafer as a function of the incident angle for both polarizations.

the same beam path to generate 2ω pulses at 400 nm (λ_2). Both beams were reflected from the silicon wafer at some incident angle, taking advantage of the fact that reflectivity of silicon varies with wavelengths and polarizations of the fundamental and second-harmonic beams (see the inset in **Figure 7**). We can control the intensity ratio $P_{2\omega}/P_{\omega}$ of the two (collinear) beams by adjusting the incident angle. A pair of wedge prisms with controllable optical path difference was used to precisely adjust the relative time delay between the ω and 2ω pulses. We also employed a 5-mm-thick β-BBO to compensate the group velocity mismatch (GVM) of the two colors in the beam path. Besides, the ω and 2ω fields with original polarizations perpendicular to each other, were passed through a dual-color zero-order wave plate serving as a half-wave plate for 800 nm to make polarizations of the two colors parallel. Finally, the ω and 2ω pulses, overlapped in time with the same linear polarizations were focused on the sample. The spatial and temporal overlap and adjustment of the phase difference between the ω and 2ω fields were conducted using a procedure described previously [14].

4. Single-color femtosecond laser ablation of PMMA

4.1. Introduction

Ultrafast laser-induced ablation or breakdown of wide band gap materials, such as polymers [1, 2, 36–41], fused silica [6], and silicon [7, 42] have already been intensively studied. Among

http://dx.doi.org/10.5772/65637

them, various kinds of polymers, such as polymethylmethacrylate (PMMA) [2, 36, 38–41], polyimide (PI) [1], polyethylene (PE) [37], polypropylene (PP), and polycarbonate (PC) [2], have drawn a lot of attention due to their potential industrial applications. Compared to ns-laser ablation, the energy ablation threshold fluence of fs-laser at approximately the same incident wavelength is known to be reduced [43]. This can be attributed to the fact that the breakdown intensities in the fs regime approach that of the threshold of multiphoton ionization of which the electron densities is high enough to cause damage [35]. On the other hand, because the induced energy absorbed by electrons is much faster than that transferred to a lattice [35]; therefore, the nonthermal ablation nature of such behavior achieved by applying fs-lasers could lead to a significant reduction of heat-affected zones. Also of interest is the possibility of decreasing the threshold for ablation. For example, Stuart et al. observed a continuously decreasing threshold with a gradual transition from the thermal regime where the longer pulses (>100 ps) dominated the ablation compared with the shorter pulses (<10 ps), which is caused by multiphoton ionization and plasma formation [17].

To date, studies of single-color femtosecond laser ablation of PMMA were overwhelmingly conducted using the Ti: sapphire laser system of which the central wavelength is around 800 nm [44–46]. On the other hand, photoablation of materials with ultraviolet (UV) lasers has also gained in popularity [36, 47–49]. The mechanism for ablation of materials by UV light is mainly through the photochemical process by one-photon absorption. Most of the dielectrics, such as glass and polymer, have relatively high absorption coefficient in the UV region. This is in contrast to the commonly accepted mechanism for ablation of PMMA using 800 nm laser pulses, such as photothermal, photophysical, or multiphoton ionization and tunneling ionization, as mentioned previously. Therefore, it is of interest to conduct a comparative study of single-color femtosecond laser ablation of PMMA using the Ti: sapphire laser and its second harmonic.

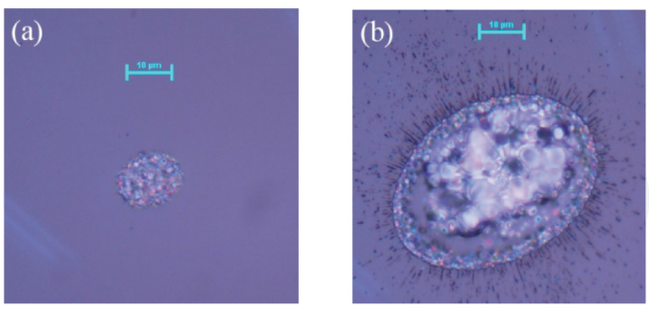

Figure 8. Images of single-color (800 nm) and single-shot ablated holes. The input laser fluence are equal to (a) 2.63 J/cm^2 and (b) 5.90 J/cm^2 , respectively.

4.2. Single-shot single-color (800 nm) femtosecond laser ablation of PMMA

In **Figure 8**, we show images of single-shot ablated holes in PMMA irradiated with femtosecond pulses at the wavelength of 800 nm. By changing the input laser fluence from 2.63 to 5.90 J/cm^2, areas of the holes are found to be equal to 155.25 and 1359.50 μm^2, respectively.

The photon energy for 800 nm is equal to 1.55 eV and the material band gap of PMMA is 4.58 eV. Therefore, more than three incident photons are needed for photoabsorption, leading to ablation. For such studies, one of the key parameter for studying the mechanism of ablation is its threshold. The method we used to define the ablation threshold value is measuring the ablated hole areas by using an optical microscope. In **Figure 9**, we have plotted hole-area of the ablated holes as a function of the irradiating laser fluence.

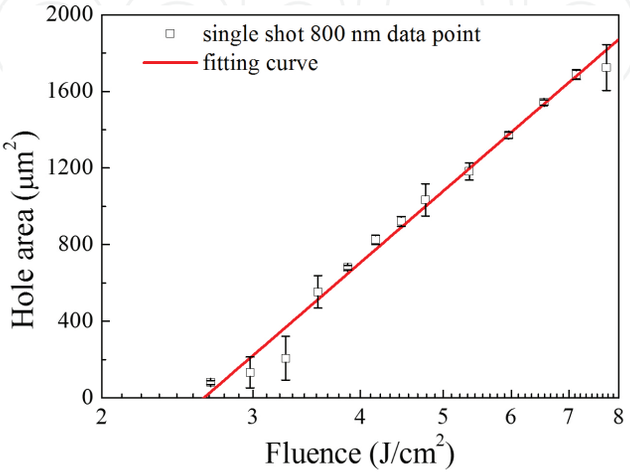

Figure 9. Hole-areas of the single-shot, single-color (800 nm) femtosecond laser ablated holes are plotted as a function of the irradiating laser fluence. Error bars are indicated.

Assuming the irradiating beam has a Gaussian spatial profile, the generally accepted scaling law for ablated holes for incident laser fluence is given by

$$D^2 = 2w^2 \ln\left(\frac{F}{F_{th}}\right) \tag{18}$$

where D is the diameter of the ablated region, w is effective laser beam width, F is the incident laser fluence and F_{th} denotes the ablation threshold (unit here is J/cm²). Following Eq. (18), the ablation threshold F_{th} can be determined by fitting the experimental data to be 2.63 J/cm².

4.3. Single-shot single-color (400 nm) femtosecond laser ablation of PMMA

To compare, we conducted similar ablation studies with exciting wavelength at 400 nm. Recall that the material band gap of PMMA is 4.58 eV, which means the dominated mechanism for photoablation on PMMA at 400 nm is also multiphoton absorption. The photon energy for 400 nm is equal to 3.1 eV. Therefore, more than two incident photons are needed for photoabsorption, leading to ablation. In **Figure 10**, we show images of single-shot ablated holes in PMMA irradiated with femtosecond pulses at the wavelength of 400 nm. By changing the input laser fluence from 1.78 to 3.92 J/cm², the hole areas are found to increase from 155.25 to 1359.50 μm², respectively.

http://dx.doi.org/10.5772/65637

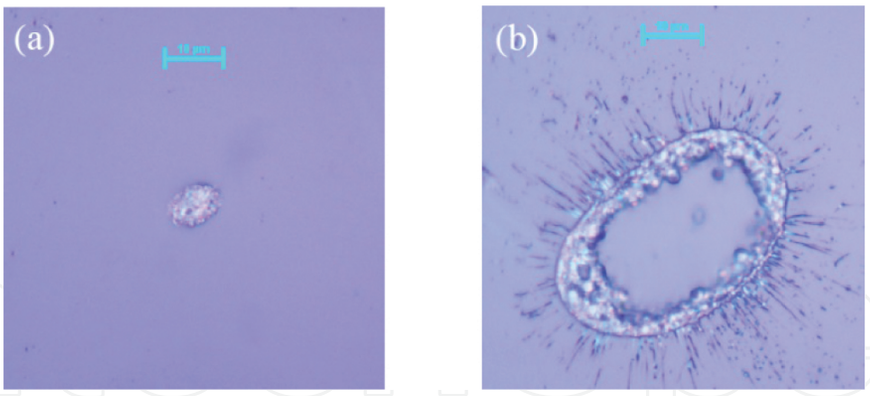

Figure 10. Images of single-color (400 nm) and single-shot ablated holes. The input laser fluence are equal to (a) 1.78 J/cm^2 and (b) 3.92 J/cm^2, respectively.

Figure 11 shows determination of the ablation threshold in the case of exciting wavelength at 400 nm. It can be seen that the same scaling behavior is observed in the case of ablation by the near IR beam. Our data show that the ablation threshold for PMMA irradiated by the near UV light of 400 nm is about 1.38 J/cm^2.

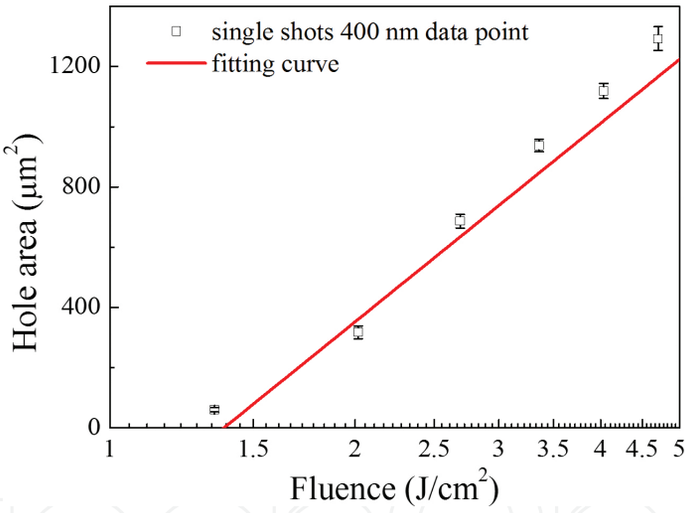

Figure 11. Single-colour ablation results for PMMA irradiated by femtosecond laser pulses with a central wavelength 400 nm. The fitted ablation threshold F_{th} is equal to 1. 38 J/cm^2.

5. Laser ablation of PMMA with femtosecond two-color synthesized waveforms

5.1. Introduction

As we noted earlier, laser ablation studies were conducted almost exclusively with single-color laser beams [6, 7, 37, 42]. There are a few studies that employed two-color lasers. These studies

can be organized into two categories: incoherent combination and coherent superposition of the two-color laser beams. An example of ablation by incoherently combined two-color beams is the work of Théberge et al., in which the authors observed an increase in volume of the ejected material by applying the superposition of fs and ns pulses. This was attributed to the free electrons and defect sites induced by the fs pulses, which could be exploited by the ns pulses [6]. Besides, Okoshi et al. reported that dual-color fs pulses with a fluence ratio of (2ω:ω = 2:78 mJ/cm^2) could etch PE deeper and faster. It was proposed that an isolated carbon, in addition to C=O and C=C–H bonds, was formed on the ablated surface after treating PMMA with 2ω or dual-color pulses. The higher photon energy of 2ω pulses then cuts the chemical bonds of PE to form the modified layer on the ablated surface [37]. In related studies of fused silica, because of the creation of defect states or free electron plasma by dual-color fs pulses at zero delay, the enhancement of absorption/reflection was observed [6]. For silicon, upon using ns and picosecond (ps)-laser pulses, it was also shown that a weak 2ω beam can be beneficial in exciting electrons into conduction band to launch the ablation process of silicon [42]. In contrast, for fs pulses, where a sufficient population on the conduction band can be created by multiphoton absorption, this effect became insignificant [42].

All the above studies employ relatively long-time delays between the two colors, on the scale of the carrier lifetime (≈ picoseconds). If the relative delay is of the order of an oscillation period between dual-color fs pulses, interesting phenomena could unfold. In other fields, a dual-color coherently superposed beams achieved by relative-phase control of each color were applied to study the physical mechanism of intense-field photoionization, especially in the gas phase [11, 24]. Schumacher et al., for example, studied the electric-field phase-dependent photoelectrons created in a regime including the multiphoton and tunneling signatures simultaneously by changing the dual-color relative phase [24]. Later, Gao et al. claimed this phase-difference effect resembled the phenomenon of quantum interference (QI) between the different channels characterized by the number of photons. In other words, phase-dependent photoemission is not a classical-wave effect, but rather a quantum-mechanical one. Recently, in comparison with monochromatic excitation, the threshold of plasma formation has been demonstrated to be significantly improved with the superposition of an ns infrared laser pulses and its second-harmonic field [11]. The authors explained their measurements by the effect of a field-dependent ionization cross section [11]. In the following, we report results of our studies of the ablation of PMMA using dual-color waveform synthesis of ω and 2ω beams of an fs Ti: sapphire laser.

5.2. Single-shot dual-color ablation of PMMA

In **Figure 12**, we show images of single-shot ablated holes in PMMA irradiated with dual-color (ω and 2ω) femtosecond pulses. In this experiment, the average powers of ω and 2ω beams are 200 and 40 mW, respectively. The corresponding laser fluence for the fundamental (NIR) beam is equal to 7.55 J/cm^2. Phase dependence of ablated holes was observed. **Figure 12(a)**, for which the relative phase $\varphi = \pi$, the ablated hole area is equal to 844.95 μm^2. When the relative phase $\varphi = 0$, area of the ablated hole is 982.31 μm^2 (see **Figure 12b**).

http://dx.doi.org/10.5772/65637

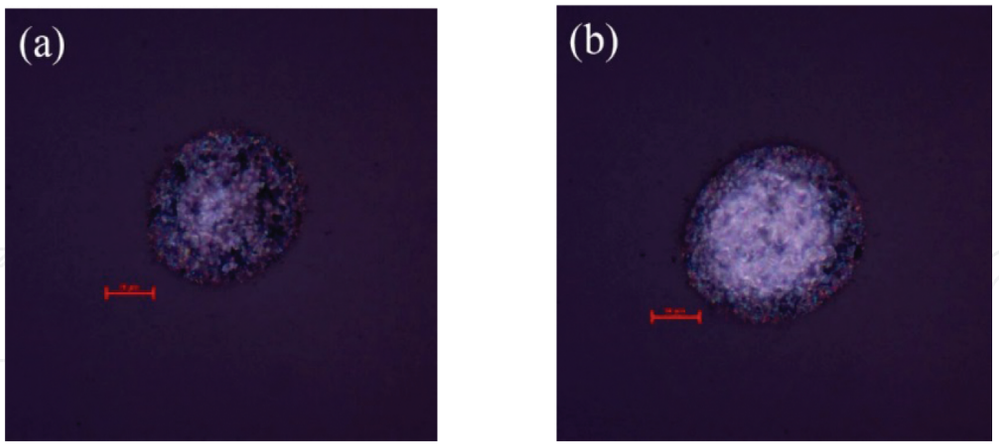

Figure 12. Images of single-shot ablated holes in PMMA irradiated by dual-colour (ω and 2ω) femtosecond lasers. The laser fluence for the fundamental beam is equal to 7.55 J/cm^2 and ratio of second-harmonic to the fundamental beams was 1:5. The hole areas of (a) 844.95 μm^2 (b) 982.31 μm^2 were observed when the relative phase φ were set to π and 0, respectively. The length of the red double-arrows in Fig. 12 (a) and (b) are both equal to 10 μm.

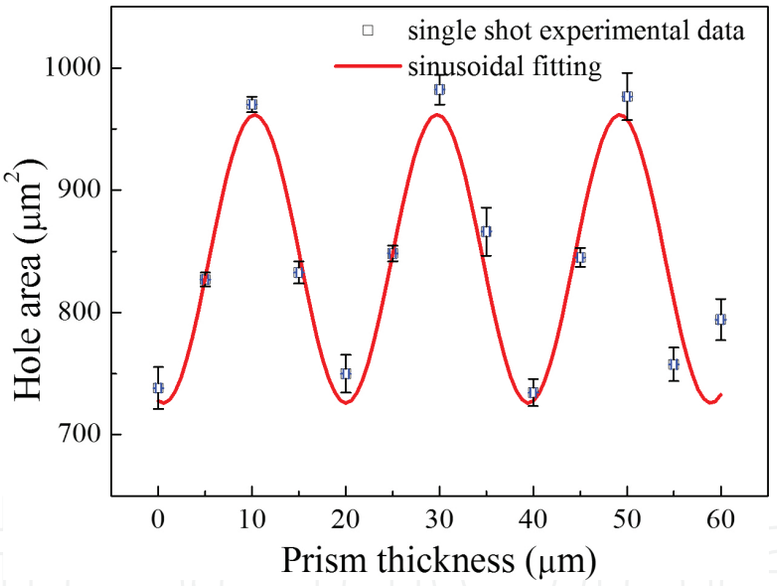

Figure 13. The ablated hole area versus relative prisms' thickness with sinusoidal fitting in the case of single shot. The period for the ablated hole areas' change is equal to 19.5 μm.

By varying the prism thickness traversed by the laser beams (see **Figure 7**), we observed that hole areas oscillated, as shown in **Figure 13**. Theoretically, we expect a sinusoidal variation with a period (relative phase change of 2π) of 20 μm. This is in good agreement with experimentally determined period of 19.5 μm in **Figure 7**.

According to our model, the two-color ionization rate would depend on the relative phase. In **Figure 14**, we have plotted the ionization rate according to Eq. (6) for synthesized dual-color instantaneous field from Eq. (7) as a function of the relative phase. The corresponding ablated

hole areas are also plotted for comparison. The difference in period between the fitting curve in **Figure 13** and the simulation curve in **Figure 14** is only 1.3%.

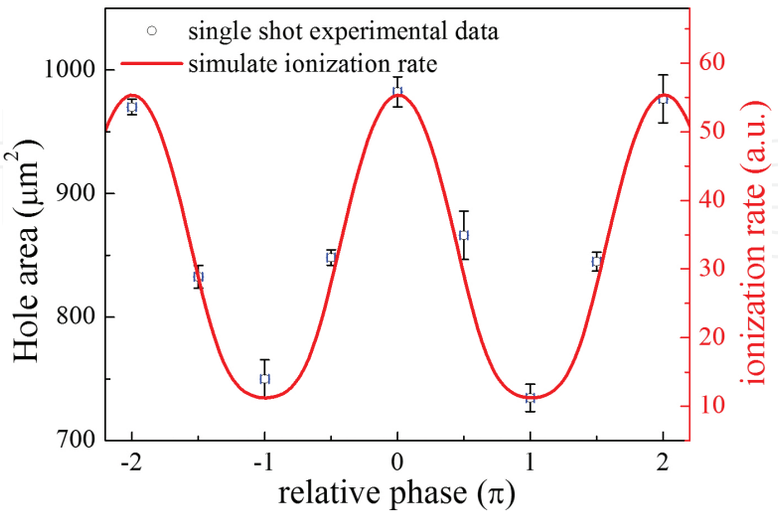

Figure 14. The ablated hole area and simulated dual-color ionization rate versus relative phase in the case of single shot. The observed modulation contrast in ablated area is ≈28% (peak to peak).

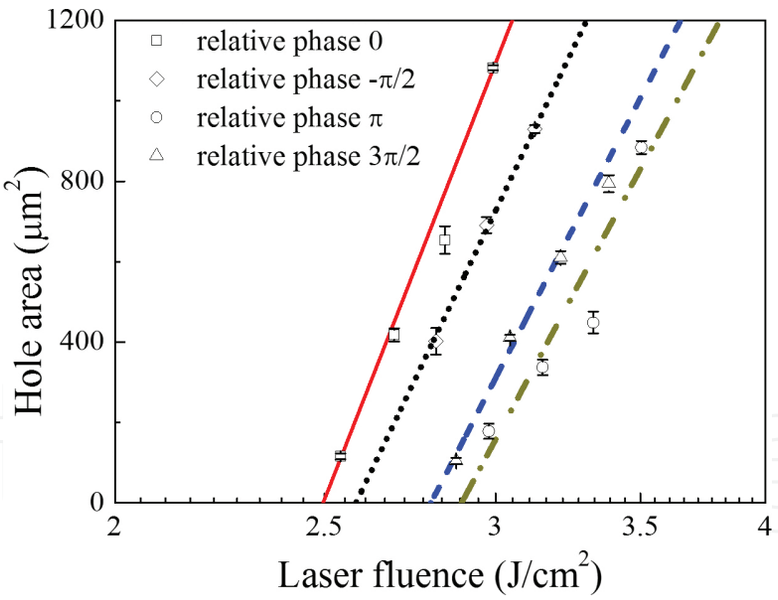

Figure 15. The ablation threshold measurement. The single-shot ablated hole areas in PMMA irradiated by femtosecond dual-color synthesized waveforms are plotted as a function of laser fluence. Four sets of data for different values of relative phases are shown.

In order to study how the relative phase affects the ablation threshold, we conducted a series of experiments in which the wedge prism's thickness was fixed at some value and the laser fluence varied. The family of experimentally measured ablated hole areas for three values of relative phase as a function or irradiating laser fluence are plotted in **Figure 15**. The same

http://dx.doi.org/10.5772/65637

scaling law for the single-color case was used to fit the experimental data. In this manner, we were able to determine the ablation threshold for a given value of relative phase. The ablation thresholds are 2.49, 2.58, 2.89 and 2.80 J/cm^2, respectively, for the relative phase to be equal to 0, $-\pi/2$, π and $3\pi/2$.

Interestingly, the fitted ablation thresholds also exhibit apparent dependence on the relative phase between ω to 2ω beams for our dual-color pulses. This is shown in **Figure 16**. The period of the sinusoidal oscillation is $\approx 2.4\pi$.

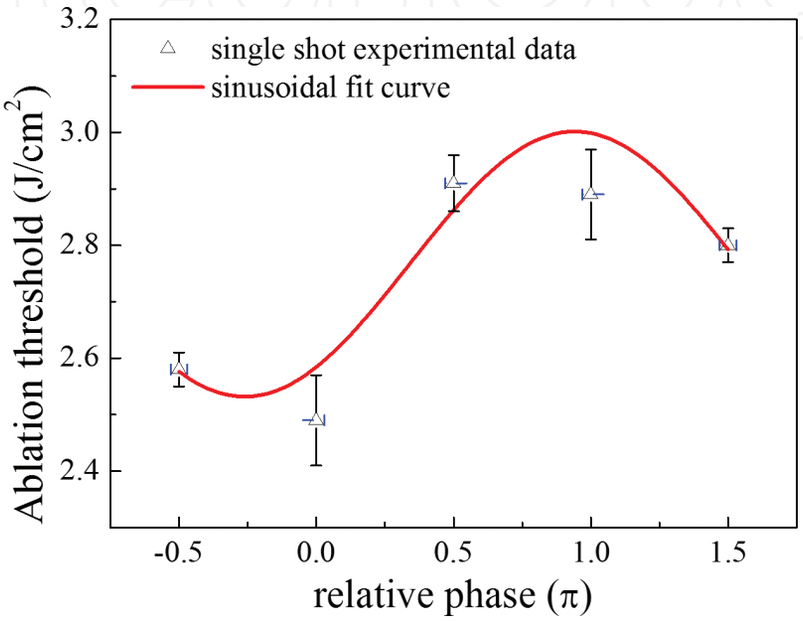

Figure 16. The ablation threshold in PMMA irradiated by femtosecond dual-color synthesized waveforms is plotted as a function of relative phase changes. The period for the ablation thresholds' change is ≈2.4π.

Because the ablation threshold is dependent upon the number of free electrons created in the material [35, 50], we believe the observed periodicity in ablation threshold in **Figure 16** demonstrates how electric field of the synthesized waveform affects the variation of ablation threshold. In the above experiments, the beam waists for every condition deliberately kept to be approximately the same. These are equal to 49.42, 54.58, 46.46, 46.69 and 47.51 μm in the cases of relative phase set at $-\pi/2$, 0, $\pi/2$, π and $3\pi/2$. That is, variation in the beam spot size is small, ±3.90%.

6. Summary

In this work, we have investigated single-shot laser ablation of polymethylmethacrylate (PMMA) using dual-color waveform synthesis of the fundamental (ω) and its second harmonic (2ω) of a femtosecond Ti: Sapphire laser. For comparison, single-color studies were also conducted. The threshold fluence for single-color ablation of PMMA irradiated by fundamental (ω) (NIR) and its second-harmonic (2ω) (NUV) beams were found to be respectively, 2.63

and 1.38 J/cm^2. Changing the relative phase of the fundamental (ω) and second-harmonic (2ω) outputs of the exciting laser resulted in clear modulation of the ablated area. The modulation as well as the ablation threshold depends on the relative phase between the ω and 2ω beams. The ablation thresholds for ablation of PMMA irradiated by two-color femtosecond frequency-synthesized waves are 2.49, 2.58, 2.89 and 2.80 J/cm^2, respectively, for the relative phase to be equal to 0, $-\pi/2$, π and $3\pi/2$. The results correlated well with the theoretical model of laser breakdown (ablation) of transparent materials through photoionization in the intermediate regime (Keldysh parameter $\gamma \approx 1.5$). Our study clearly illustrates the potential applications of using phase-controlled synthesized waveform for laser processing of materials.

Acknowledgements

This work was funded by the grant of the National Science Council 102-2622-E-007-021-CC2, 101-2221-E-007-103-MY3, and 101-2112-M-007-019-MY3. The authors would like to thank Dr. Wei-Jen Chen for many useful discussions. They would also like to thank Prof. Ru-Pin Pan for the use of the microscope.

Author details

Ci-Ling Pan[1,2,3*], Chih-Hsuan Lin[2], Chan-Shan Yang[1,4] and Alexey Zaytsev[1]

*Address all correspondence to: clpan@phys.nthu.edu.tw

1 Department of Physics, National Tsing Hua University, Hsinchu, Taiwan

2 Institute of Photonics Technology, National Tsing Hua University, Hsinchu, Taiwan

3 Frontier Research Center on Fundamental and Applied Sciences of Matters, National Tsing Hua University, Hsinchu, Taiwan

4 Department of Physics, University of California, Berkeley, CA, USA

References

[1] S. Baudach, J. Bonse, and W. Krautek, "Ablation experiments on polyimide with femtosecond laser pulses," Applied Physics A-Materials Science & Processing, 69, S395–S398 (1999).

http://dx.doi.org/10.5772/65637

[2] S. Baudach, J. Bonse, J. Kruger, and W. Kautek, "Ultrashort pulse laser ablation of polycarbonate and polymethylmethacrylate," Applied Surface Science, 154–155, 555–560 (2000).

[3] P.P. Rajeev, M. Gertsvolf, E. Simova, C. Hnatovsky, R.S. Taylor, V.R. Bhardwaj, D.M. Rayner, and P.B. Corkum, "Memory in nonlinear ionization of transparent solids," Physical Review Letters, 97, 253001-1-5 (2006).

[4] N. Sanner, O. Uteza, B. Bussiere, G. Coustillier, A. Leray, T. Itina, and M. Sentis, "Measurement of femtosecond laser-induced damage and ablation thresholds in dielectrics," Applied Physics A-Materials Science & Processing, 94, 889–897(2009).

[5] Y.P. Deng, X.H. Xie, H. Xiong, Y.X. Leng, C.F. Cheng, H.H. Lu, R.X. Li, and Z.Z. Xu, "Optical breakdown for silica and silicon with double femtosecond laser pulses," Optics Express, 13(8), 3096–3103 (2005).

[6] I.H. Chowdhury, X. Xu, and A.M. Weiner, "Ultrafast two-color ablation of fused silica," Applied Physics A-Materials Science & Processing, 83, 49–52 (2006).

[7] S. Zoppel, R. Merz, J. Zehetner, and G.A. Reider, "Enhancement of laser ablation yield by two color excitation," Applied Physics A-Materials Science & Processing, 81, 847–850 (2005).

[8] T.J. Derrien, T. Sarnet, M. Sentis, and T.E. Itina, "Application of a two-temperature model for the investigation of the periodic structure formation on Si surface in femtosecond laser interactions," Journal of Optoelectronics and Advanced Materials, 12(3), 610–615 (2010).

[9] M.D. Perry, B.C. Stuart, P.S. Banks, M.D. Feit, V. Yanovsky, and A.M. Rubenchik, "Ultrashort-pulse laser machining of dielectric materials," Journal of Applied Physics, 85(9), 6803–6810 (1999).

[10] B. Chimier, O. Uteza, N. Sanner, M. Sentis, T. Itina, P. Lassonde, F. Legare, F. Vidal, and J.C. Kieffer, "Damage and ablation thresholds of fused-silica in femtosecond regime," Physical Review B, 84, 094104-1-10 (2011).

[11] E. Schwarz and G.A. Reider, "Laser-induced plasma by two-color excitation," Applied Physics B-Lasers and Optics, 107(1), 23–30 (2012).

[12] X. He, J.M. Dahlstrom, R. Rakowski, C.M. Heyl, A. Persson, J. Mauritsson, and A. L'Huillier, "Interference effects in two-color high-order harmonic generation," Physical Review A, 82, 033410 (2010).

[13] X. Xie, J. Dai, and X. C. Zhang, "Coherent control of THz wave generation in ambient air," Physical Review Letters, 96, 075005-1-4 (2006).

[14] C.-S. Yang, C.-H. Lin, A. Zaytsev, K.-C. Teng, T.-H. Her, and C.-L. Pan, "Femtosecond laser ablation polymethylmethacrylate via dual-color synthesized waveform," Applied Physics Letters, 106, 051902-1-5 (2015).

[15] S.R. Cain, "A photothermal model for polymer ablation: chemical modification," Journal of Physical Chemistry, 97, 051902-1-5(1993).

[16] R.R. Gattass and E. Mazur, "Femtosecond laser micromachining in transparent materials," Nature Photonics, 2, 219–225 (2008).

[17] B.C. Stuart, M.D. Feit, A.M. Rubenchik, B.W. Shore, and M.D. Perry, "Laser-induced damage in dielectrics with nanosecond to subpicosecond pulses," Physical Review Letters, 74(12), 2248–2251 (1995).

[18] M. Lenzner, J. Kruger, S. Sartania, Z. Cheng, C. Spielmann, G. Mourou, W. Kautek, and F. Krausz, "Femtosecond optical breakdown in dielectrics," Physical Review Letters, 80(18), 4076–4079 (1998).

[19] M. Li, S. Menon, J.P. Nibarger, and G.N. Gibson, "Ultrafast electron dynamics in femtosecond optical breakdown of dielectrics," Physical Review Letters, 82(11), 2394–2397 (1999).

[20] D.W. Schumacher, F. Weihe, H.G. Muller, and P.H. Bucksbaum, "Phase dependence of intense field ionization: a study using two colors," Physical Review Letters, 73(10), 1344–1347 (1994).

[21] R.M. Potvliege and P.H.G. Smith, "2-Color multiphoton ionization of hydrogen by an intense laser field and one of its harmonics," Journal of Physics B: Atomic and Molecular Physics, 25, 2501–2516 (1992).

[22] P.B. Corkum, N.H. Burnett, and F. Brunel, "Above-threshold ionization in the long-wavelength limit," Physical Review Letters, 62(11), 1259–1262 (1989).

[23] A.C. Tien, S. Backus, H. Kapteyn, M. Murnane, and G. Mourou, "Short-pulse laser damage in transparent materials as a function of pulse duration," Physical Review Letters, 82(19), 3883–3886 (1999).

[24] D.W. Schumacher and P.H. Bucksbaum, "Phase dependence of intense-field ionization," Physical Review A, 54(5), 4271–4278 (1996).

[25] R. Sauerbrey and G.H. Pettit, "Theory for the etching of organic materials by ultraviolet laser pulses," Applied Physics Letters, 55(5), 421–423 (1989).

[26] A.V. Sokolov, D.R. Walker, D.D. Yavuz, G.Y. Yin, and S.E. Harris, "Femtosecond light source for phase-controlled multiphoton ionization," Physical Review Letters, 87(3), 033402-1-4 (2001).

[27] H. Kumagai, K. Midorikawa, K. Toyoda, S. Nakamura, T. Okamoto, and M. Obara, "Ablation of polymer films by femtosecond high-peak-power Ti: sapphire laser at 798 nm," Applied Physics Letters, 65(14), 1850–1852 (1994).

[28] G.H. Pettit and R. Sauerbrey, "Pulsed ultraviolet laser ablation," Applied Physics A-Materials Science & Processing, 56, 51–63 (1993).

[29] C.B. Schaffer, A. Brodeur, and E. Mazur, "Laser-induced breakdown and damage in bulk transparent materials induced by tightly focused femtosecond laser pulses," Measurement Science & Technology, 12, 1784–1794 (2001).

[30] S.C. Jones, P. Braunlich, R.T. Casper, X.A. Shen, and P. Kelly, "Recent progress on laser-induced modifications and intrinsic bulk damage of wide-gap optical materials," Optical Engineering, 28, 1039–1068 (1989).

[31] L.V. Keldysh, "Ionization in field of a strong electromagnetic wave," Soviet Physics JETP-USSR, 20(5), 1307 (1965).

[32] P. Balling and J. Schou, "Femtosecond-laser ablation dynamics of dielectrics: basics and applications for thin films," Reports on Progress in Physics, 76(3), 39 (2013).

[33] M.J. DeWitt and R.J. Levis, "Calculating the Keldysh adiabaticity parameter for atomic, diatomic, and polyatomic molecules," The Journal of Chemical Physics, 108(18), 7739–7742 (1998).

[34] T. Brabec and F. Krausz, "Nonlinear optical pulse propagation in the single-cycle regime," Physical Review Letters, 78(17), 3282 (1997).

[35] B.C. Stuart, M.D. Feit, S. Herman, A.M. Rubenchik, B.W. Shore, and M.D. Perry, "Nanosecond-to-femtosecond laser-induced breakdown in dielectrics," Physical Review B, 53(4), 1749–1761 (1996).

[36] R. Srinivasan, "Ablation of polymers and biological tissue by ultraviolet-lasers," Science, 234(4776), 559–565 (1986).

[37] M. Okoshi and N. Inoue, "Laser ablation of polymers using 395 nm and 790 nm femtosecond lasers," Applied Physics A-Materials Science & Processing, 79(4–6), 841–844 (2004).

[38] J.R. Nam, K.S. Lim, and S.C. Jeoung, "Femtosecond laser ablation of polymethylmethacrylate doped with dye molecules and formation of a grating structure," Journal of the Korean Physical Society, 52(5), 1661–1664 (2008).

[39] D. Klinger, R. Sobierajski, R. Nietubyc, J. Krzywinski, J. Pelka, L. Juha, M. Jurek, D. Zymierska, S. Guizard, and H. Merdji, "Surface modification of polymethylmethacrylate irradiated with 60 fs single laser pulses," Radiation Physics and Chemistry, 78, S71–S74 (2009).

[40] J.M. Guay, A. Villafranca, F. Baset, K. Popov, L. Ramunno, and V.R. Bhardwaj, "Polarization-dependent femtosecond laser ablation of poly-methyl methacrylate," New Journal of Physics, 14, 085010 (2012).

[41] F. Baset, K. Popov, A. Villafranca, J.M. Guay, Z. Al-Rekabi, A.E. Pelling, L. Ramunno, and R. Bhardwaj, "Femtosecond laser induced surface swelling in poly-methyl methacrylate," Optics Express, 21(10), 12527–12538 (2013).

[42] S. Zoppel, J. Zehetner, and G.A. Reider, "Two color laser ablation: enhanced yield, improved machining," Applied Surface Science, 253(19), 7692–7695 (2007).

[43] S. Kuper and M. Stuke, "Femtosecond UV excimer laser ablation," Applied Physics B-Photophysics and Laser Chemistry, 44(4), 199–204 (1987).

[44] P.J.S. Alexandra Baum, W. Perrie, M. Sharp, K.G. Watkins, D. Jones, R. Issac, and D.A. Jaroszynski, "NUV and NIR femtosecond laser modification of PMMA," LPM20007 - The 8th International Symposium on Laser Precision Microfabrication, pp. 1–5 (2007).

[45] A.A. Serafetinides, M. Makropoulou, E. Fabrikesi, E. Spyratou, C. Bacharis, R.R. Thomson, and A.K. Kar, "Ultrashort laser ablation of PMMA and intraocular lenses," Applied Physics A-Materials Science & Processing, 93(1), 111–116 (2008).

[46] C. De Marco, S.M. Eaton, R. Suriano, S. Turri, M. Levi, R. Ramponi, G. Cerullo, and R. Osellame, "Surface properties of femtosecond laser ablated PMMA," ACS Applied Materials & Interfaces, 2(8), 2377–2384 (2010).

[47] H. Schmidt, J. Ihlemann, B. Wolff-Rottke, K. Luther, and J. Troe, "Ultraviolet laser ablation of polymers: spot size, pulse duration, and plume attenuation effects explained," Journal of Applied Physics, 83(10), 5458–5468 (1998).

[48] S. Lazare and V. Granier, "Ultraviolet-laser photoablation of polymers – a review and recent results," Laser Chemistry, 10(1), 25–40 (1989).

[49] R. Srinivasan, E. Sutcliffe, and B. Braren, "Ablation and etching of polymethylmethacrylate by very short (160 fs) ultraviolet (308 nm) laser-pulses," Applied Physics Letters, 51(16), 1285–1287 (1987).

[50] B.C. Stuart, M.D. Feit, S. Herman, A.M. Rubenchik, B.W. Shore, and M.D. Perry, "Optical ablation by high-power short-pulse lasers," Journal of the Optical Society of America B-Optical Physics, 13(2), 459–468 (1996).